ACS OMEGA

http://pubs.acs.org/journal/acsodf

Article

New Type of Catalyst for Efficient Aerobic Oxidative Desulfurization Based On Tungsten Carbide Synthesized by the Microwave Method

Argam V. Akopyan,* Raman A. Mnatsakanyan, Ekaterina A. Eseva, David A. Davtyan, Polina D. Polikarpova, Maxim O. Lukashov, Ivan S. Levin, Kirill A. Cherednichenko, Alexander V. Anisimov, Anna M. Terzyan, Artur M. Agoyan, and Eduard A. Karakhanov

Cite This: *ACS Omega* 2022, 7, 11788−11798

Read Online

ACCESS | Metrics & More | Article Recommendations | Supporting Information

ABSTRACT: Herein, we present a new type of high-performance catalyst for aerobic oxidation of organosulfur compounds based on tungsten carbide. The synthesis of tungsten carbide was performed via microwave irradiation of the precursors, which makes it possible to obtain a catalyst in just 15 min. The synthesized catalyst was investigated by a variety of physicochemical methods: X-ray diffraction, X-ray photoelectron spectroscopy, Raman spectroscopy, electron microscopy, and N_2 adsorption/desorption. It was shown that active centers containing tungsten in the transition oxidation state (+4) play a key role in the activation of oxygen. The main factors influencing the conversion of dibenzothiophene (DBT) were investigated. It should be noted that 100% conversion of DBT can be achieved under relatively mild conditions: 120 °C, 3 h, 6 bar, and 0.5% wt catalyst. The catalyst retained its activity for at least six oxidation/regeneration cycles. The simplicity and speed of synthesis of the proposed catalyst in combination with its high activity and stability open broad prospects for its further use both for oxidative desulfurization and for other reactions of aerobic oxidation of organic substrates.

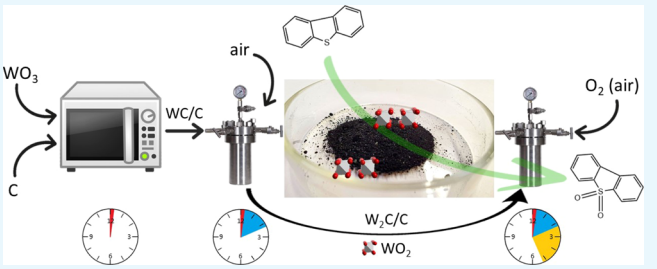

1. INTRODUCTION

The growth in energy consumption and the associated increase in crude oil production lead to the need of developing new fields, in which the quality of the oil produced is steadily declining. Sulfur content is one of the key indicators of oil quality because sulfur compounds are among the main components of oil that pollute the environment.[1] The trend toward an increase in the sulfur content in the produced hydrocarbon feedstock calls for the development of existing as well as the emergence of new technologies that would make it possible to obtain petroleum products with low and ultra-low sulfur content with a minimal negative impact on the environment.[2] The existing hydrotreating technology allows one to essentially reduce the sulfur content in the refined petroleum products. However, the implementation of this technology requires high capital costs and elevated temperatures and pressures, which are inaccessible for small oil refineries. At the same time, a significant amount of elemental sulfur is formed as a byproduct of hydrotreating. The industrial demand for such byproducts is lower than their production rate, which leads to the accumulation of elemental sulfur and harms the environment.[3]

Thus, today, it is urgent to search for alternative non-hydrogen methods to reduce the sulfur content in oil products, allowing efficient desulfurization with minimal waste generation. The following anhydrous methods are known from the literature: extraction,[4,5] adsorption,[6,7] biodesulfurization,[8,9] and oxidative desulfurization.[10−13] Among these alternative approaches, the method of oxidative desulfurization attracts the greatest interest of researchers because of this technique's capability of reducing the sulfur content in various petroleum fractions down to ultra-low values with sufficiently high selectivity.[14] In this case, the reaction products, sulfones, can be selectively recovered and used in various industries and agriculture.[15,16]

The number of works in the field of oxidative desulfurization has recently increased significantly.[10,17] It should be noted that in most works, environmentally friendly hydrogen peroxide is used as an oxidizing agent, which yields water as the byproduct of its reduction.[18,19] However, an increase in the sulfur content in the feed requires significant volumes of this oxidant, which increases the cost of such purification and complicates the practical implementation of this approach to oxidative desulfurization. Therefore, using air oxygen as an oxidant

Received: December 9, 2021
Accepted: March 22, 2022
Published: April 1, 2022

appears to be the most viable approach to the development of novel oxidative desulfurization techniques.

The key issue for the use of air as an oxidizing agent is finding a catalyst that would allow the selective oxidation of sulfur-containing compounds in a hydrocarbon environment. A wide variety of catalysts were suggested in the literature for aerobic oxidative desulfurization.[20,21] In particular, molybdenum oxides modified with zinc and cobalt oxides can be used for aerobic oxidation of sulfur-containing compounds.[22,23] The catalysts are fairly easy to synthesize and permit removing more than 80% of sulfur compounds. The key disadvantage of such systems is the high reaction temperature of 350 °C, which, on the one hand, increases the energy consumption and, on the other hand, leads to the formation of toxic sulfur dioxide. Complexes of metals, in particular phthalocyanines of iron and cobalt, allow reducing the sulfur content in the model mixture of dibenzothiophene (DBT) by 90%.[24−26] However, phthalocyanines are difficult to synthesize, which negatively affects the cost of purification. Polyoxometalates have proven themselves as active catalysts for the aerobic oxidation of sulfur-containing compounds, which, under relatively mild conditions (temperatures up to 150 °C), allow the exhaustive oxidation of DBT.[27,28] However, such catalysts as polyoxometalates require laborious synthesis procedures. Catalysts containing noble metals are highly active;[29−32] however, the high cost of such catalysts complicates their practical application.

Nanoporous tungsten oxide containing pentavalent tungsten in addition to the hexavalent one has been successfully used recently as a catalyst for aerobic oxidation.[33] The presence of defects in the catalyst structure, as well as tungsten in an intermediate oxidation state, made this catalyst highly efficient for the oxidation of DBT and dimethyldibenzothiophene under mild conditions (temperature, 120 °C). It was shown for the first time in this work that tungsten in an intermediate oxidation state enables the activation of air oxygen with the formation of a superoxide radical. This opens up wide opportunities for the synthesis of tungsten-containing catalysts for aerobic oxidative desulfurization of petroleum fractions.[34,35]

It is known that the oxidation of tungsten to oxides occurs on the surface of tungsten carbide in air. In particular, ref 36 shows the presence of the WO_2 phase on the surface of tungsten carbide. This fact, taking into account the known literature data, suggests that tungsten carbide can potentially catalyze aerobic oxidation reactions.

Tungsten carbide was widely used for a long time due to its unique properties.[37] In particular, tungsten carbide can act as an effective catalyst for chemical reactions that traditionally occur in the presence of noble metals such as platinum or palladium.[38] Recently, interest in tungsten carbide has been growing due to its use as a catalyst for the oxidation of methanol[39] and electro-oxidation of hydrogen.[40−42] However, pure tungsten carbide is synthesized at high temperatures and using a laborious procedure, which negatively affects the cost of such a catalyst.

In this work, tungsten carbide deposited on activated carbon was obtained via microwave synthesis. This method allows producing the catalyst in just 15 min. We have shown for the first time that tungsten carbide-based catalysts thus obtained can be successfully applied for aerobic oxidative desulfurization, allowing the efficient removal of various classes of organosulfur compounds under mild conditions. This simple, highly efficient, and, at the same time, rapidly synthesized catalyst opens broad prospects for developing novel approaches to aerobic oxidative desulfurization.

2. EXPERIMENTAL SECTION

2.1. Catalyst Preparation. Pure tungsten oxide (WO_3) and carbon powder (Vulcan XC-72R, Cabot Co) were used as the precursors for the synthesis of WC. Carbon served as both a precursor for obtaining tungsten carbide[43] and as the thermal reducer because carbon is highly efficient at absorbing microwave energy and converting it into heat. A stoichiometric ratio of the elements in the initial mixture was calculated based on the $WO_3 + 4C = WC + 3CO$ equation. The mixture of powders containing 11.8 g of WO_3 and 2.45 g of C (2.5 wt % higher than stoichiometric ratio) was weighed and carefully mixed in a quartz cup for 2 h using a magnetic stirrer. Afterward, the mixture was placed in a quartz flow reactor for better degasifying. A quartz lid containing tubes for gas inlets and outlets was mounted at the top of the reactor, which was then purged with 25 mL/min flow of high purity (99.999%) helium at room temperature for 2 h.[44,45] Once the reaction mixture settled at the bottom of the quartz reactor at the completion of degasifying, a tube was inserted vertically into an oven through an opening. To avoid rapid reaction and strong gas release, the reactor with the mixture was irradiated at 900 W in five successive steps at 5, 10, 20, and 30 s. Subsequently, the mixture was subjected to microwave heating at 900 W to white-hot glowing for 900 s. The average temperature of microwave heating was measured to be 1150 °C by an infrared thermometer (Dostman HT 1800). Continuously flowing helium was used to protect the materials from oxidation during the synthesis. During cooling, the gas flow was kept for 2 h. Then, the product was kept inside the reactor at room temperature for 24 h for the deactivation of the surface.

2.1.1. Activation Procedure. The calculated amount of the WC/C catalyst was loaded into a steel autoclave equipped with a magnetic stirrer. Then, the autoclave was hermetically sealed and pumped with air to a pressure of 6 atm. The autoclave was immersed in an oil bath heated to 120 °C, stirring at 600 rpm was activated, and the whole was kept thus for 2 h. Then, the autoclave was cooled and the activated catalysts were used for further experiments.

2.2. Catalytic Experiments. The oxidation reaction was carried out in a 40 mL steel autoclave. The autoclave was loaded with 26 mg of the catalyst (0.5 wt %), 6 mL of a model solution of a sulfur-containing substrate in decalin with a sulfur content of 500 ppm, and a stirrer. Next, the air was pumped in to achieve the required pressure. The autoclave was heated in an oil bath to the reaction temperature. The reaction was carried out with constant stirring at 600 rpm for 2 h. Then, the autoclave was cooled in cold water to room temperature, opened, and the sample was removed. Reaction products were analyzed by GC-FID with an absolute calibration method [Kristall 2000 M equipped with a capillary column (ZB-1 liquid phase, 30 m × 0.32 mm)]. The data thus obtained were used to calculate the conversion degree of the substrate via the following equation

$$\eta = [(C_0 - C_t)/C_0] \times 100\%$$

where C_0 and C_t are the initial concentration of DBT in the oil phase and that taken at time t, respectively.

2.3. Characterizations. X-ray phase analysis was performed on a Rigaku Rotaflex D/max-RC instrument using copper Cu Kα-radiation (λ = 0.154 nm). The diffraction

https://doi.org/10.1021/acsomega.1c06969
ACS Omega 2022, 7, 11788−11798

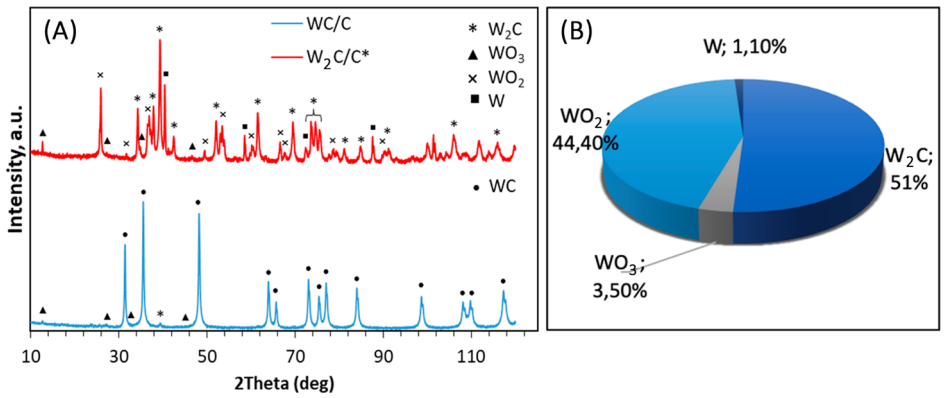

Figure 1. XRD pattern of samples (A) and quantitative analysis from profile-fitted peaks of W_2C/C^* (B).

pattern from the sample was registered in the angular range 2θ = 10−120° with a step of 0.02° and a recording rate of 2°·min^{-1}. Quantitative phase analysis was carried out by the corundum number method using the MDI JADE program.

The sample crystal structure was studied with the help of high-resolution transmission electron microscopy (HRTEM) using a transmission electron microscope JEOL JEM-2100 UHR. The sample suspensions were dropped onto Lacey formvar/carbon films on copper TEM grids (Ted Pella, Inc). The accelerating voltage was set to 200 kV. The morphology of the samples was investigated by scanning electron microscopy (SEM) employing a dual beam scanning electron microscope JEOL JIB-4501. The fine sample powders were fixed on the carbon tape and sputtered by a 10 nm carbon layer. The SEM micrographs were acquired in the 15−30 kV accelerating voltage range. The chemical composition of the samples were explored with the help of energy-dispersive spectroscopy (EDS) using an EX-24065JGT EDS spectrometer (JEOL).

IR spectra of diffuse reflectance (DRIFT) were obtained using a high-temperature PIKE Diffus IR cell coupled to a VERTEX-70 Fourier transform infrared (FTIR) spectrometer. The spectra were recorded in the range 600−4000 cm^{-1} with a resolution of 40 cm^{-1} (100 scans/spectrum).

The N_2 adsorption−desorption isotherms at 77 K were investigated using a Gemini VII 2390 (V1.02t) surface area and porosity analyzer (Micromeritics Instrument). Before measurements, the samples were degassed at a temperature of 120 °C for 6 h. The surface area was calculated by the Brunauer−Emmett−Teller (BET) method based on adsorption data in the range of relative pressures P/P_0 = 0.05−0.2. The total pore volume was determined based on the amount of adsorbed nitrogen at a relative pressure P/P_0 = 0.95. The volume of micropores was determined using the *t*-plot method.

The Raman spectra were recorded on a Horiba LabRAM HR Evolution spectrometer. To excite the Raman spectra, a HeCd laser with a wavelength of 633 nm was used. Spectral resolution was 3 cm^{-1}.

X-ray photoelectron spectroscopy (XPS) spectra of the surface layers were recorded on an OMICRON ESCA + spectrometer (OMICRON, Germany). The pressure in the chamber of the OMICRON ESCA + analyzer was maintained below 8 × 10^{-10} mbar, the radiation source was the Al anode (Al Kα 1486.6 eV).

3. RESULTS AND DISCUSSION

The target catalyst was synthesized in two stages. At the first stage, tungsten carbide WC/C was obtained using the microwave method, which reduces the synthesis time to 15 min. In the second stage, activation was carried out by oxidizing the obtained carbide with atmospheric oxygen to obtain target catalyst W_2C/C^*, which contains tungsten oxide in an intermediate oxidation state.

3.1. Catalyst Characterization. The X-ray diffraction (XRD) patterns of the tungsten carbide samples are shown in Figure 1. The patterns for the synthesized WC/C contained mainly diffraction peaks from tungsten monocarbide (WC) with low-intensity signals of tungsten dicarbide and hydrotungstite. Peaks at the 2θ of 31.46, 35.6, 48.26, 63.98, 73.04, 75.44, 77.06, 84.02, 98.06, 108.1, 109.7, and 117.28° correspond to the reflections of the WC crystal.[46,47] The XRD pattern of the W_2C/C^* sample activated by oxidation includes mixed phases of tungsten sub-carbide (W_2C), tungsten (W), tungsten dioxide (WO_2), and hydrotungstite ($H_2WO_4{\cdot}H_2O$). The diffraction peaks at the 2θ of 34.36, 37.92, 39.38, 52.14, 61.56, 69.52, 73.64, 74.62, 75.62, 81.12, 84.94, and 91.18° were attributed to the diffraction planes of W_2C; the peaks at 2θ = 12.76, 27.34, 36.28, and 46.62° were related to monoclinic hydrotungstite; 2θ = 40.46, 58.58, 72.46, and 87.58° corresponded to crystalline tungsten. The diffraction peaks at 2θ = 25.96, 35.9−37.9, 52.9−53.9, 60.2, 66.6−68.9, 79.32, and 81.22° are the characteristic monoclinic tungsten (IV) oxide reflection.[48,49] Figure 1B presents the content of the detected phases in the W_2C/C^* powder. The contents of the W_2C and WO_2 phases in the synthesized samples were 51 and 44.4%, respectively.

The Raman spectra of WC/C and W_2C/C^* are presented in Figure 2. Several peaks were detected at 133, 270, 324, 651,

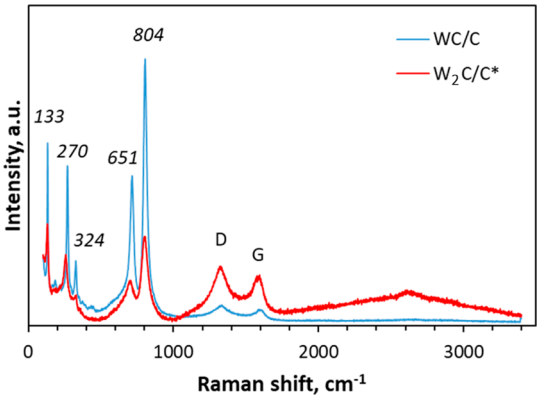

Figure 2. Raman spectra of the samples.

https://doi.org/10.1021/acsomega.1c06969
ACS Omega 2022, 7, 11788−11798

804, 1322, and 1584 cm^{-1}. The latter two peaks are attributed to the carbon phase in the samples. The peak located at 1322 cm^{-1} corresponds to graphite (G band) and 1584 cm^{-1} can be ascribed to disordered graphite (D band).[36,47] The G band corresponds to the E_{2g} vibration of graphitic carbon with an sp^2 electronic configuration, whereas the D band is associated with the A_{1g} mode of the diamond-like carbon with an sp^3 configuration.[50] Besides, the spectra showed the presence of tungsten carbide and oxide phase in the samples. The peaks at 804 cm^{-1} are associated with W−C stretching modes, and the rest of the peaks can be attributed to the W−O stretching and bending modes of the oxide phase of tungsten.[33,51] All the Raman spectroscopy data are in a good agreement with those obtained from the XRD pattern.

As shown in Figure 3, the synthesized and activated samples have type II isotherm with a H1 type hysteresis loop, which

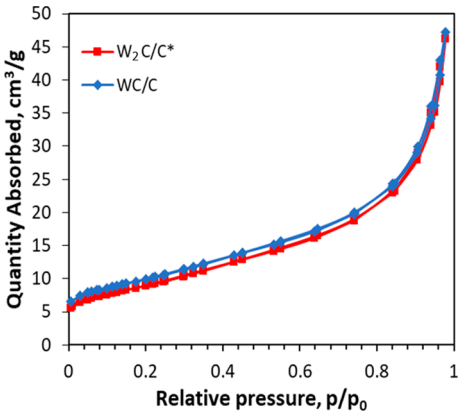

Figure 3. Nitrogen adsorption−desorption isotherm of the samples.

indicates the presence of tubular capillaries with different shapes, opened at both ends or to the formation of a porous network.[52] It should be noted that the BET surface area was 14 m^2/g for the synthesized WC/C and decreased slightly to 12 m^2/g for the activated sample (W_2C/C^*). This means that the phase transition during the activation occurs on the surface of the carbon support and does not affect the texture characteristics of the initial sample (Table 1).

Table 1. Textural Properties of the Catalyst Samples

sample	BET surface area, m^2/g	total pore volume, cm^3/g	pore size, nm
WC/C	14	0.038	10
W2C/C*	12	0.036	10

The surface morphologies of the tungsten carbide powders were obtained via SEM micrographs. As can be seen in Figure 4, the samples have a grainy structure with an average grain size of approximately 50−90 nm.[53] The composition of the samples was analyzed from EDS (Figure 4I,F). The WC/C samples contained two elements (W and C), whereas the activated W_2C/C^* contained oxygen in addition to tungsten and carbon. This result indicates the presence of tungsten oxide in the composition of the sample, which was confirmed by HRTEM. A comprehensive analysis of the WC/C crystal revealed the {012} set of crystallographic planes of WC, whereas in the case of W_2C^*/C crystals, the {111} set of WO_2 crystallographic planes was observed (Figure S1, Supporting Information). Thus, the results obtained from electron microscopy are in a good agreement with the XRD data.

Figure 5 shows the FTIR analysis of the samples using the DRIFT setup. Peaks at 1269 and 1186 cm^{-1} are attributed to the stretching vibration W−C, two peaks at 839 and 898 cm^{-1} are ascribed to the vibrational stretching modes of tungsten oxide W═O, and the peak at 746 cm^{-1} corresponds to O−W−O stretching vibrations.[54−56] The spectra of the activated sample contain a peak at 1083 cm^{-1}, which can be due to the stretching vibrational modes of W−C in the hexagonal crystalline structure.[57] Besides, DRIFT was used for the determination of functional groups on the carbon surfaces. Note that the peak at 1421 cm^{-1} can be ascribed to the bending vibrations of O−H bonds, whereas that at 1541 cm^{-1} can be attributed to the vibration of quinone groups, and the peak centered at 1654 cm^{-1} can correspond to the stretching vibration of C═C bonds.[58,59]

In addition, the synthesized and the activated samples were analyzed by XPS to study its chemical composition and electronic structure. According to the results of XPS studies, the sample of W_2C/C^* is composed of the elements O, C, and W (Figure S2, Supporting Information). Figure 6 shows W 4f (A, B), C 1s (C, D), and O 1s (E, F) spectra decomposed into components for the studied samples. The spectrum is a combination of three states of tungsten with the binding energies of the W $4f_{7/2}$ peaks close to 31.9 (W1), 32.9 (W2), and 36.1 (W3) eV for the synthesized sample and 31.7 (W1), 33.6 (W2), and 36.1 (W3) eV for the activated sample. According to the literature data, the W1 form can be associated with the metallic tungsten or tungsten in the composition of WC_x carbide.[60−62] The W3 state can be attributed to oxidized tungsten W^{6+} (presumably, in the composition of WO_3).[62−64] The W2 state is an intermediate and can be partially oxidized tungsten (e.g., W^{4+}) in the composition of WO_2 oxide or WO_xC_y tungsten oxycarbide. It is important to note that after the activation procedure, the surface layer of the tungsten carbide sample changes. A comparison of the two spectra shows that after oxidation the content of tungsten in the form of carbide significantly reduced (from 60 to 19%), and the amount of oxidized forms of tungsten also increases. The distribution of tungsten forms is presented in Table 2. The carbon spectra can be divided into three components: C−C, C−H with a binding energy of 285 eV, C−O 286 eV, and WC with a maximum of 283 eV; these states were also observed in refs 65 and 66. The intensity of the carbon components C−O increases in the activated sample, which indicates the partial oxidation of carbon during the activation process. The O 1s profile has three states: adsorbed water with a binding energy of 533 eV, carbon components of 532 eV, and oxide forms of tungsten with a binding energy of 531 eV. These results are in a good agreement with DRIFT and Raman spectroscopy.

It should be noted that tungsten carbide WC/C, for which trace amounts of oxides were found according to XRD data, according to the XPS spectrum, contains 31.5% tungsten in the +6 oxidation state (Table 2). In addition, in the case of the activated sample, the proportion of WO_3 species is estimated at more than 70% in XPS, while in XRD it is only 3.5%. Thus, the fraction of tungsten particles estimated from PXRD is very different from the fraction from XPS. A large difference in the content of various forms of tungsten according to the results of XRD and XPS is observed for both activated carbide and fresh tungsten carbide, and this is due to the fact that the XPS method provides information on the valence states of the

https://doi.org/10.1021/acsomega.1c06969
ACS Omega 2022, 7, 11788−11798

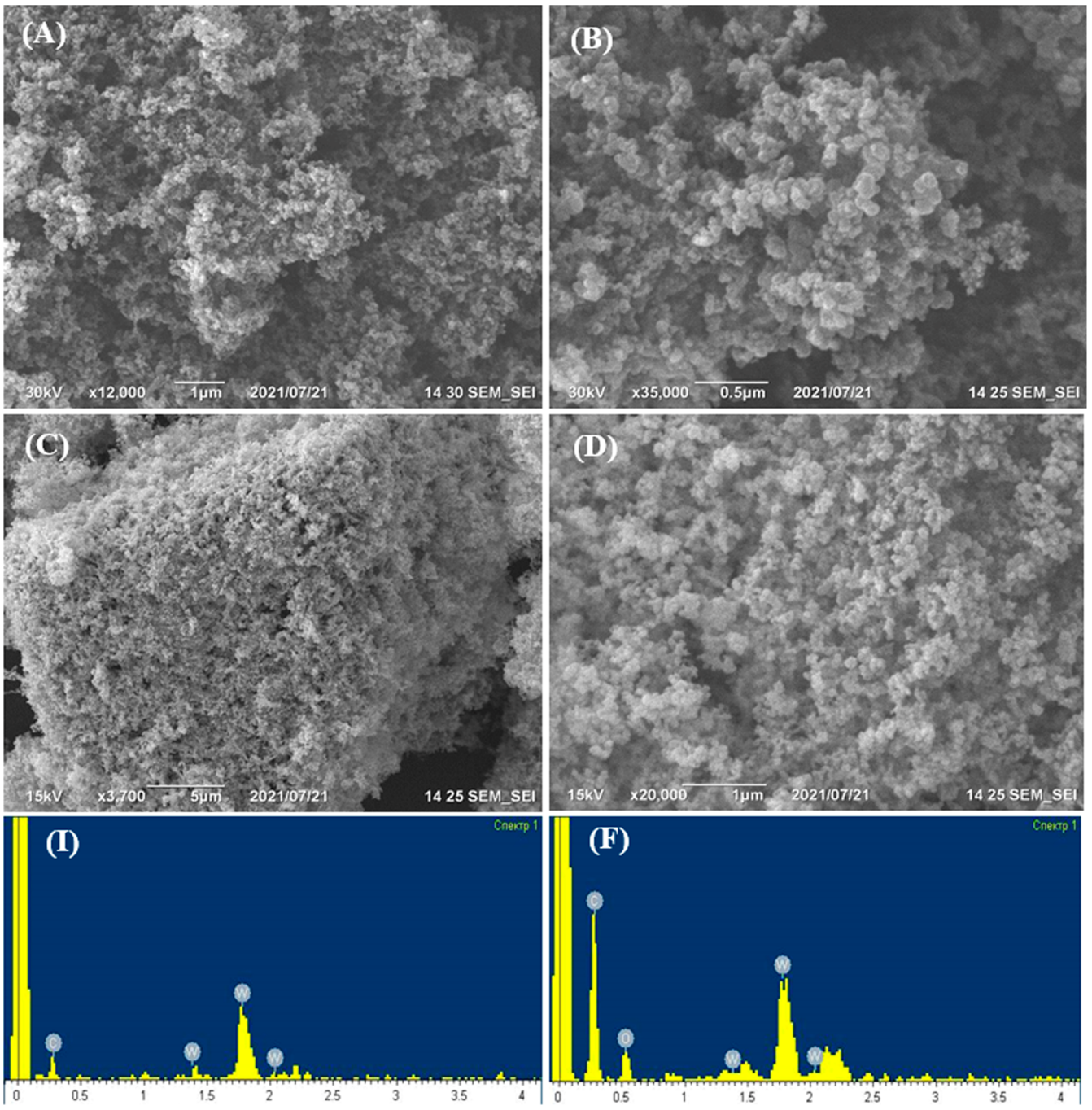

Figure 4. SEM micrographs and EDS spectra of WC/C (A,B,I) and W_2C/C* (C,D,F).

element on the sample surface. That is, the surface of the carbide contains a significant amount of oxidized forms of tungsten, which may be due to oxidation in air during storage. At the same time, the oxidation of the catalyst in air has little effect on the phase composition.

3.2. Oxidation of Model Sulfides. The activity of the catalyst was tested in aerobic oxidation of a model mixture containing DBT as an organosulfur substrate. This substrate is relatively inert toward oxidation reactions, which makes a model of choice in most studies of oxidative desulfurization described in the literature. The oxidation reactions were carried out in steel autoclaves under air pressure. The catalysts used were tungsten carbide synthesized by the microwave method (WC/C), tungsten carbide activated via oxidation (W_2C/C*), and tungsten oxide WO_3. The results obtained are shown in Figure 7.

The results obtained indicate that only activated tungsten carbide exhibits a significant catalytic activity in the aerobic oxidation of DBT. At the same time, the carbide synthesized by the microwave method without activation (WC/C) shows results worse than the control experiment. This effect possibly indicates that tungsten is oxidized under the reaction conditions, which leads to the consumption of the oxidant and reduces the rate of substrate oxidation. It should be noted that tungsten oxide WO_3 has practically no activity in aerobic oxidation; in the presence of tungsten oxide (VI), the conversion degree of DBT is close to that observed in the control experiment without a catalyst. Note that under the

https://doi.org/10.1021/acsomega.1c06969
ACS Omega 2022, 7, 11788−11798

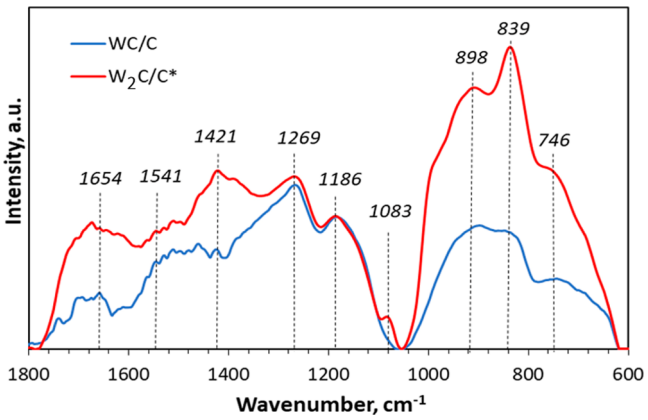

Figure 5. FTIR diffuse reflectance spectrum of WC/C and W_2C/C*.

conditions of the experiment in the presence of carbon, the results are somewhat worse than the control experiment, which can apparently be associated with the decay of the radicals formed on the surface of the carbon, which may be related to the process of carbon oxidation by the formed radical particles.[67] The results of the experiment involving carbon show that the metal center—tungsten plays a key role in the oxidation of the sulfur compound. This once again emphasizes the importance of tungsten in an intermediate oxidation state for the activation of oxygen. Because the activated carbide contains such form of tungsten, according to the results of the XPS and XRD, further experiments were carried out for the W_2C/C* catalyst.

Varying the amount of the catalyst shows that an increase in its dosage leads to an increase in DBT conversion (Figure 8). Note that in the initial part of the kinetic curve (reaction time 1 h), the DBT conversion is higher for low dosages, which indicates an increase in the induction period with an increase in the amount of catalyst. This fact, apparently, is associated with the decay of the formed radicals in the presence of tungsten carbide, which can be oxidized under these conditions. Therefore, the optimal dosage is 0.5% by weight of the catalyst, which ensures exhaustive oxidation of DBT in 3 h. Based on the data obtained, the apparent rate constants and activation energy (165.5 kJ/mol) were calculated (Figure S3, Supporting Information).

Data on DBT conversion under different reaction temperatures are shown in Figure 9.

According to the results obtained, the conversion drops sharply with decreasing temperature, which is in a good agreement with the literature data.[46] This effect is due to the activation of atmospheric oxygen which occurs at temperatures above 110 °C. A decrease in temperature below 100 °C is impractical because of the low reaction rate. A rise in temperature above 120 °C is also undesirable due to the possible occurrence of side reactions of oxidation of hydrocarbon components. Therefore, a temperature of 120 °C is optimal because this is the minimum temperature at which it is possible to achieve exhaustive oxidation of DBT.

We have also studied the effect of air pressure on the conversion of DBT (Figure 10). Note that at a minimum pressure of 2 bar, the oxidant/sulfur molar ratio is 17:1, whereas for the complete oxidation of DBT, a twofold excess of the oxidant is sufficient. In this case, according to the results on varying the pressure, the DBT conversion increases with increasing pressure from 2 to 6 bar, which is associated with an increase in the solubility of oxygen in hydrocarbon fractions with increasing pressure. This allows us to assume that only oxygen dissolved in the model fuel takes part in the oxidation reaction. A further increase in pressure to 10 bar leads only to an insignificant increase in the DBT conversion, which can be associated with the saturation of the model mixture with dissolved oxygen.

The activity of various classes of organosulfur substrates decreases in the series methylphenylsulfide (MeSPh) > methyldibenzothiophene (MeDBT) > DBT > dimethyldibenzothiophene (Me_2DBT) > benzothiophene (BT), which is in a good agreement with the literature data[68] and is associated with two main factors: the electron density on the sulfur atom, as well as steric hindrances (Figure 11).

It is known from the literature that the addition of radical traps to the system makes it possible to determine how oxygen is activated.[69] In particular, it was shown[33] that active centers consisting of tungsten in an intermediate oxidation state can activate oxygen by forming a superoxide radical. The formation of this radical was confirmed by the addition of benzoquinone, which is a well-known superoxide radical trap, to the system. In this work, we carried out the oxidation of a model DBT mixture with the addition of benzoquinone (Figure 12). The presence of potassium iodide slightly affects the oxidation of DBT, reducing the conversion to 53%, which may also indicate the possible formation of hydroxyl radicals during the oxidation process. The addition of sodium azide to the reaction system does not affect the oxidation of DBT.

According to the results obtained, the addition of benzoquinone to the system leads to a sharp decrease in the degree of DBT conversion, which in turn indicates that the formation of superoxide radicals is the main mechanism involved in DBT oxidation. The results obtained on the presence of tungsten in a transitional oxidation state, as well as on the activation of oxygen through the superoxide radical, are in a good agreement with the literature data.[33]

To determine the possibility of reusing the synthesized catalyst after the reaction, the activated tungsten carbide was separated by centrifugation, washed with acetone from the formed sulfone, dried at a temperature of 80 °C under reduced pressure, and used to oxidize a fresh portion of the model fuel. The results are shown in Figure 13.

Note that no significant change in the activity of the catalyst is observed upon reuse, which indicates the possibility of applying the synthesized catalyst in a batch mode. The spent catalyst after 6 cycles of oxidation was analyzed with XPS, XRD, and IR, and the corresponding results were added to the Supporting Information (Figures S4−S6). We would like to note that after the oxidation, the phase composition of the catalyst practically did not change and according to the XPS data, the changes in the ratios of tungsten in different oxidation states were also insignificant. The X-ray pattern of the spent catalyst is identical to the activated sample. In accordance with the IR, the spectrum of the spent catalyst has a similar set of peaks corresponding to vibrations in the bond of both tungsten carbides and oxides, and the carbon support of the catalyst. Thus, significant changes in the catalyst's composition and structure occur during activation, whereas no such changes are observed upon the oxidation of model mixtures. This also indicates the stability of the catalyst in the process of aerobic oxidative desulfurization and the preservation of its active sites.

Table 3 shows the data on aerobic oxidation of organosulfur substrates in the presence of tungsten and vanadium-

https://doi.org/10.1021/acsomega.1c06969
ACS Omega 2022, 7, 11788−11798

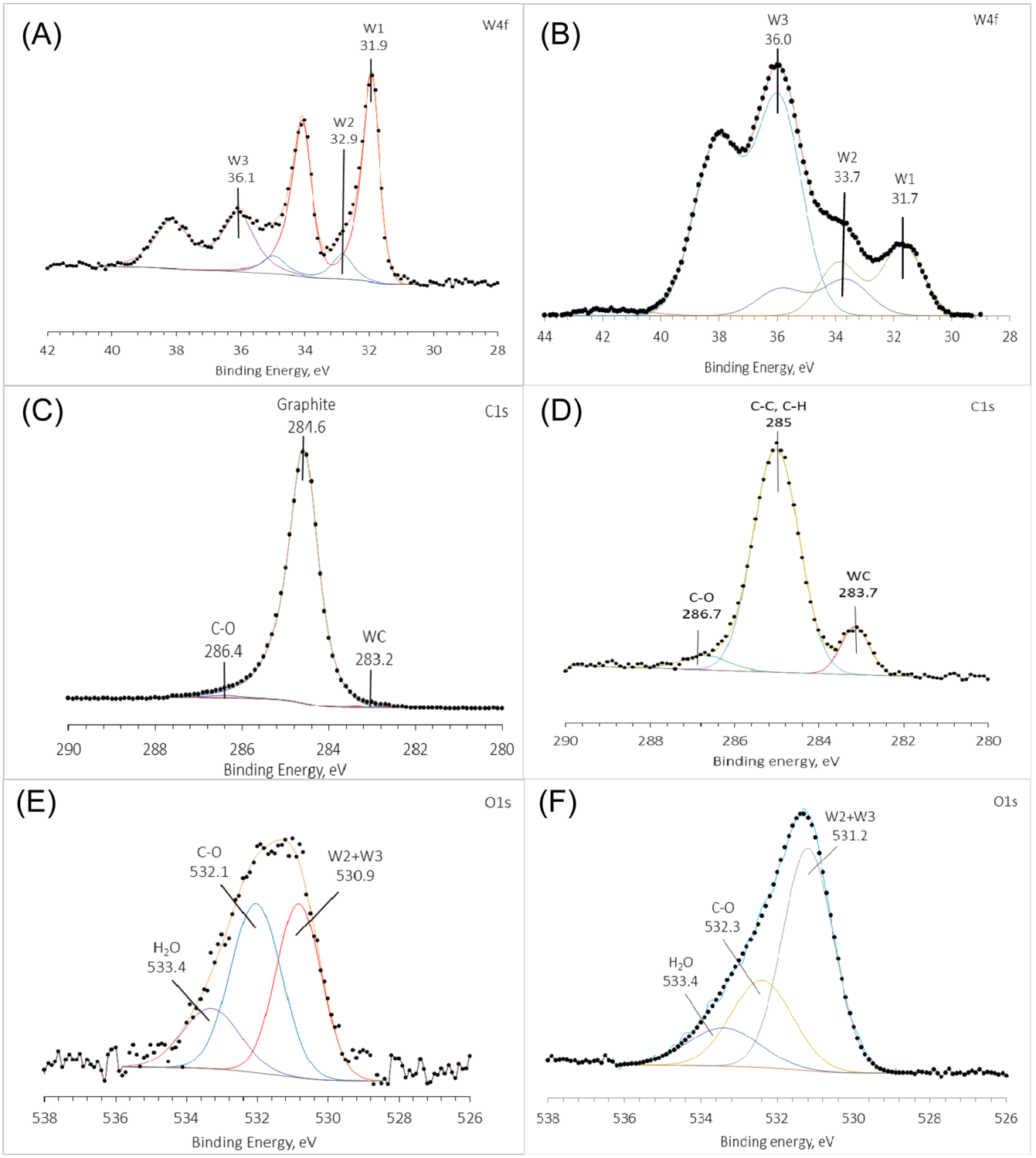

Figure 6. XPS spectra of W 4f (A,B), C 1s (C,D), and O 1s (E,F) regions of WC/C (A,C,E) and W_2C/C* (B,D,F) catalysts.

Table 2. Distribution of Tungsten forms on the Surface of the W_2C/C* Catalysts

	tungsten forms, quant., at. %		
catalyst	W1	W2	W3
WC/C	60.5	8	31.5
W2C/C*	19	11	70

containing catalysts. It should be noted that there are few works in the literature on the use of tungsten oxides for the process of aerobic oxidative desulfurization. Among the studied catalytic systems, the catalyst synthesized in the present work makes it possible to reduce the time required to achieve 100% DBT conversion to 3 h at a temperature of 120 °C. It is also significant that the synthesis of the catalyst studied in the work takes only 15 min and the activation stage lasts 2 h. This result

https://doi.org/10.1021/acsomega.1c06969
ACS Omega 2022, 7, 11788−11798

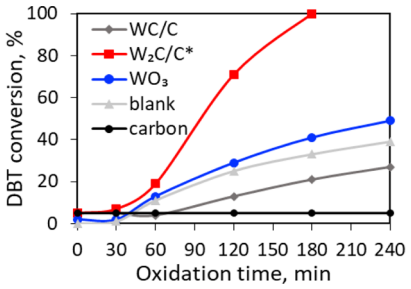

Figure 7. Activity of catalysts in aerobic oxidation of DBT. Oxidation conditions: 120 °C, the catalyst dosage 0.5 wt %, 6 bar.

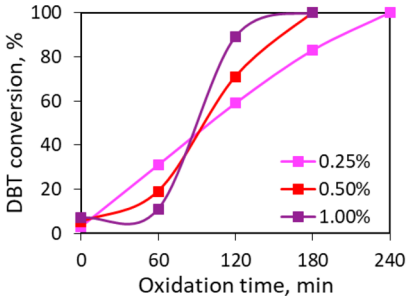

Figure 8. Effect of catalyst amount on DBT conversion. Oxidation conditions: 120 °C, W_2C/C^* catalyst, 6 bar.

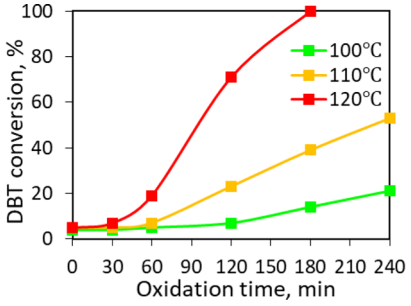

Figure 9. Effect of reaction temperature on DBT conversion. Oxidation conditions: W_2C/C^* catalyst, 0.5 wt %, 6 bar.

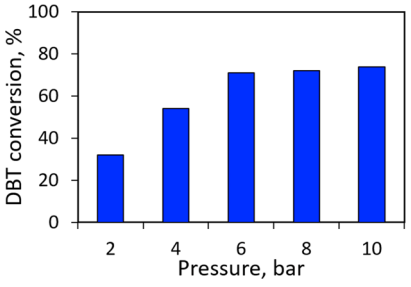

Figure 10. Effect of air pressure on DBT conversion. Oxidation conditions: W_2C/C^* catalyst, 0.5 wt %, 120 °C, 2 h.

is unattainable for the currently known catalytic systems, all of which take a much longer time to synthesize.

CONCLUSIONS

Tungsten carbide was synthesized using the microwave method, which provides the possibility of rapid synthesis (up to 15 min) and does not require the presence of hydrogen and methane. An original method for the activation of tungsten carbide is proposed, which makes it possible to obtain tungsten

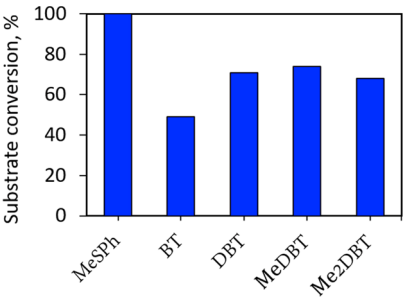

Figure 11. Oxidation of various sulfur-containing substrates. Conditions: catalyst (W_2C/C^*) 0.5 wt %, 120 °C, 6 bar.

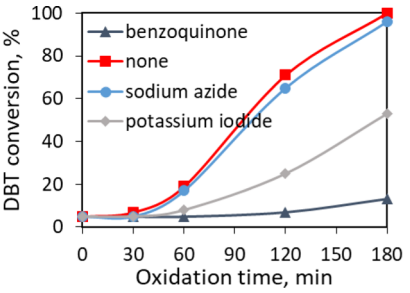

Figure 12. Role of radical trap on DBT conversion. Oxidation conditions: W_2C/C^* catalyst, 0.5 wt %, 120 °C, 6 bar.

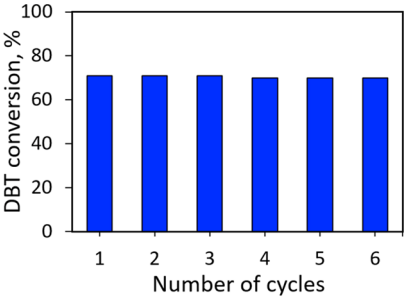

Figure 13. Oxidation of DBT with a regenerated catalyst. Oxidation conditions: W_2C/C^* catalyst, 0.5 wt %, 120 °C, 6 bar, 2 h.

in an intermediate oxidation state. The resulting catalyst was characterized by a variety of physicochemical methods. According to XRD and XPS data, the catalyst contains tungsten in the intermediate oxidation state of +4 in the form of WO_2 oxide, which is capable of activating atmospheric oxygen. Analysis of the data of low-temperature adsorption/desorption of nitrogen showed that oxidation of tungsten carbide does not lead to a significant change in the textural characteristics of the catalyst.

The influence of the main factors on the conversion of DBT in the presence of the synthesized catalyst has been studied in detail. The optimal temperature, which allows to achieve the exhaustive oxidation of DBT was determined. It was shown that the air pressure has a significant effect on the results obtained, which suggests that the oxidation reaction involves mainly oxygen dissolved in the model fuel. The addition of a radical trap, benzoquinone, to the system leads to a sharp drop in the degree of DBT conversion, which indicates that the activation of oxygen through the formation of superoxide radicals plays a key role in oxidative desulfurization with this novel catalyst. Under optimal conditions, it is possible to achieve 100% conversion of DBT: reaction time 3 h, air

https://doi.org/10.1021/acsomega.1c06969
ACS Omega 2022, 7, 11788−11798

Table 3. Comparison of Metal-Containing Catalysts for Aerobic Oxidative Desulfurization[a]

catalyst	substrate	temperature, °C	time, min	conversion, %	references
3DOM WO*x*-400	4,6-Me2DBT	120	240	99.0	33
MFM-300(V)	DBT	120	300	99.6	70
V_2O_5/BNNS	DBT	120	240	99.6	71
WO_3/MMS-500	DBT	120	480	99.9	35
W_2C/C*	DBT	120	180	100	this work

[a]DOM—three-dimensional ordered macro−mesoporous. MMS—magnetic mesoporous core−shell structure.

pressure 6 bar, catalyst weight content 0.5%, and temperature 120 °C.

The synthesized W_2C/C* catalyst shows high stability and retains its activity for at least six oxidation/regeneration cycles. The simplicity of the synthesis of this catalyst, the availability of components for synthesis, high activity, and stability open broad prospects for its further application both for oxidative desulfurization and for other reactions of aerobic oxidation of organic substrates.

■ ASSOCIATED CONTENT

Supporting Information

The Supporting Information is available free of charge at https://pubs.acs.org/doi/10.1021/acsomega.1c06969.

HRTEM images, XPS spectra, pseudo-first-order kinetic curves, X-ray pictures, and FTIR diffuse reflectance spectrum (PDF)

■ AUTHOR INFORMATION

Corresponding Author

Argam V. Akopyan − *Chemistry Department, Lomonosov Moscow State University, Moscow 119234, Russia;* orcid.org/0000-0001-6386-0006; Phone: +7 (495) 939-36-66; Email: arvchem@yandex.ru

Authors

Raman A. Mnatsakanyan − *A. B. Nalbandyan Institute of Chemical Physics National Academy of Sciences of Armenia, Yerevan 0014, Armenia*

Ekaterina A. Eseva − *Chemistry Department, Lomonosov Moscow State University, Moscow 119234, Russia;* orcid.org/0000-0001-7538-9012

David A. Davtyan − *A. B. Nalbandyan Institute of Chemical Physics National Academy of Sciences of Armenia, Yerevan 0014, Armenia*

Polina D. Polikarpova − *Chemistry Department, Lomonosov Moscow State University, Moscow 119234, Russia;* orcid.org/0000-0002-0456-8248

Maxim O. Lukashov − *Chemistry Department, Lomonosov Moscow State University, Moscow 119234, Russia;* orcid.org/0000-0002-4656-6232

Ivan S. Levin − *A. V. Topchiev Institute of Petrochemical Synthesis, 119991 Moscow, Russia;* orcid.org/0000-0002-0800-575X

Kirill A. Cherednichenko − *Department of Physical and Colloid Chemistry, Gubkin University, Moscow 119991, Russia;* orcid.org/0000-0002-1868-8232

Alexander V. Anisimov − *Chemistry Department, Lomonosov Moscow State University, Moscow 119234, Russia;* orcid.org/0000-0001-9272-2913

Anna M. Terzyan − *A. B. Nalbandyan Institute of Chemical Physics National Academy of Sciences of Armenia, Yerevan 0014, Armenia*

Artur M. Agoyan − *A. B. Nalbandyan Institute of Chemical Physics National Academy of Sciences of Armenia, Yerevan 0014, Armenia*

Eduard A. Karakhanov − *Chemistry Department, Lomonosov Moscow State University, Moscow 119234, Russia;* orcid.org/0000-0003-4727-954X

Complete contact information is available at: https://pubs.acs.org/10.1021/acsomega.1c06969

Author Contributions

All authors contributed equally. The manuscript was written through the contributions of all authors. All authors have approved the final version of the manuscript.

Funding

The reported study was funded by RFBR and SC RA, project number 20-58-05002.

Notes

The authors declare no competing financial interest.

■ ABBREVIATIONS

BET, Brunauer−Emmett−Teller
BT, benzothiophene
DBT, dibenzothiophene
DRIFT, IR spectra of diffuse reflectance
EDS, energy-dispersive spectroscopy
FTIR, Fourier transform infrared spectroscopy
MeBT, 5-methylbenzothiophene
MeDBT, 4-methyldibenzothiophene
Me_2DBT, 4,6-dimethyldibenzothiophene
ODS, oxidative desulfurization methods
SEM, scanning electron microscopy
XPS, X-ray photoelectron spectroscopy
XRD, X-ray diffraction

■ REFERENCES

(1) Demirbas, A.; Alidrisi, H.; Balubaid, M. A. API gravity, sulfur content, and desulfurization of crude oil. *Pet. Sci. Technol.* **2015**, *33*, 93−101.

(2) Julião, D.; Gomes, A.; Cunha-Silva, L.; Valença, R.; Ribeiro, J. C.; Pillinger, M.; de Castro, B.; Gonçalves, I. S.; Balula, S. S. A sustainable peroxophosphomolybdate/H_2O_2 system for the oxidative removal of organosulfur compounds from simulated and real high-sulfur diesels. *Appl. Catal., A* **2020**, *589*, 117154.

(3) Lim, J.; Pyun, J.; Char, K. Recent approaches for the direct use of elemental sulfur in the synthesis and processing of advanced materials. *Angew. Chem., Int. Ed.* **2015**, *54*, 3249−3258.

(4) Babich, I.; Moulijn, J. A. Science and technology of novel processes for deep desulfurization of oil refinery streams: A review. *Fuel* **2003**, *82*, 607−631.

(5) Bakar, W. A. W. A.; Ali, R.; Kadir, A. A. A.; Mokhtar, W. N. A. W. Effect of transition metal oxides catalysts on oxidative desulfurization of model diesel. *Fuel Process. Technol.* **2012**, *101*, 78−84.

(6) Sarda, K. K.; Bhandari, A.; Pant, K. K.; Jain, S. Deep desulfurization of diesel fuel by selective adsorption over Ni/Al_2O_3 and Ni/ZSM-5 extrudates. *Fuel* **2012**, *93*, 86−91.
(7) Shahadat Hussain, A. H. M.; Tatarchuk, B. J. Adsorptive desulfurization of jet and diesel fuels using Ag/TiO_x-Al_2O_3 and Ag/TiO_x-SiO_2 adsorbents. *Fuel* **2013**, *107*, 465−473.
(8) Li, F.; Zhang, Z.; Feng, J.; Cai, X.; Xu, P. Biodesulfurization of DBT in tetradecane and crude oil by a facultative thermophilic bacterium Mycobacterium goodii X7B. *J. Biotechnol.* **2007**, *127*, 222−228.
(9) Yu, B.; Xu, P.; Shi, Q.; Ma, C. Deep desulfurization of diesel oil and crude oils by a newly isolated Rhodococcus erythropolis strain. *Appl. Environ. Microbiol.* **2006**, *72*, 54−58.
(10) Houda, S.; Lancelot, C.; Blanchard, P.; Poinel, L.; Lamonier, C. Oxidative Desulfurization of Heavy Oils with High Sulfur Content: A Review. *Catalysts* **2018**, *8*, 344−369.
(11) Akopyan, A. V.; Polikarpova, P. D.; Arzyaeva, N. V.; Anisimov, A. V.; Maslova, O. V.; Senko, O. V.; Efremenko, E. N. Model fuel oxidation in the presence of molybdenum-containing catalysts based on SBA-15 with hydrophobic properties. *ACS Omega* **2021**, *6*, 26932−26941.
(12) Zhang, T.; Zhang, J.; Wang, Z.; Liu, J.; Qian, G.; Wang, D.; Gong, X. Review of electrochemical oxidation desulfurization for fuels and minerals. *Fuel* **2021**, *305*, 121562.
(13) Crucianelli, M.; Bizzarri, B. M.; Saladino, R. SBA-15 anchored metal containing catalysts in the oxidative desulfurization process. *Catalysts* **2019**, *9*, 984.
(14) Akopyan, A. V.; Kulikov, L. A.; Polikarpova, P. D.; Shlenova, A. O.; Anisimov, A. V.; Maximov, A. L.; Karakhanov, E. A. Metal-free oxidative desulfurization catalysts based on porous aromatic frameworks. *Ind. Eng. Chem. Res.* **2021**, *60*, 9049−9058.
(15) Matavos-Aramyan, S.; Soukhakian, S.; Jazebizadeh, M. H. Selected methods for the synthesis of sulfoxides and sulfones with emphasis on oxidative protocols. *Phosphorus, Sulfur Silicon Relat. Elem.* **2020**, *195*, 181−193.
(16) Hossain, M.; Park, H.; Choi, H. A Comprehensive review on catalytic oxidative desulfurization of liquid fuel oil. *Catalysts* **2019**, *9*, 229.
(17) Lim, X. B.; Ong, W.-J. A current overview of the oxidative desulfurization of fuels utilizing heat and solar light: from materials design to catalysis for clean energy. *Nanoscale Horiz.* **2021**, *6*, 588−633.
(18) Polikarpova, P.; Akopyan, A.; Shlenova, A.; Anisimov, A. New mesoporous catalysts with Bronsted acid sites for deep oxidative desulfurization of model fuels. *Catal. Commun.* **2020**, *146*, 106123.
(19) Das, S. P.; Boruah, J. J.; Sharma, N.; Islam, N. S. New polymer-immobilized peroxotungsten compound as an efficient catalyst for selective and mild oxidation of sulfides by hydrogen peroxide. *J. Mol. Catal. A: Chem.* **2012**, *356*, 36−45.
(20) Shafiq, I.; Shafique, S.; Akhter, P.; Ishaq, M.; Yang, W.; Hussain, M. Recent breakthroughs in deep aerobic oxidative desulfurization of petroleum refinery products. *J. Cleaner Prod.* **2021**, *294*, 125731.
(21) Eseva, E. A.; Akopyan, A. V.; Anisimov, A. V.; Maksimov, A. L. Oxidative desulfurization of hydrocarbon feedstock using oxygen as oxidizing agent (a review). *Pet. Chem.* **2020**, *60*, 979−990.
(22) Shi, Y.; Liu, G.; Zhang, B.; Zhang, X. Oxidation of refractory sulfur compounds with molecular oxygen over a Ce−Mo−O catalyst. *Green Chem.* **2016**, *18*, 5273.
(23) Yashnik, S. A.; Salnikov, A. V.; Kerzhentsev, M. A.; Saraev, A. A.; Kaichev, V. V.; Khitsova, L. M.; Ismagilov, Z. R.; Yamin, J.; Koseoglu, O. R. Effect of the nature of sulfur compounds on their reactivity in the oxidative desulfurization of hydrocarbon fuels with oxygen over a modified CuZnAlO catalyst. *Kinet. Catal.* **2017**, *58*, 58−72.
(24) Zhou, X.; Li, J.; Wang, X.; Jin, K.; Ma, W. Oxidative desulfurization of dibenzothiophene based on molecular oxygen and iron phthalocyanine. *Fuel Process. Technol.* **2009**, *90*, 317−323.
(25) Chen, S.; Lu, W.; Yao, Y.; Chen, H.; Chen, W. Oxidative desulfurization of dibenzothiophene with molecular oxygen catalyzed by carbon fiber supported iron phthalocyanine. *React. Kinet., Mech. Catal.* **2014**, *111*, 535−547.
(26) Buck, T.; Bohlen, H.; Wöhrle, D.; Schulz-Ekloff, G.; Andreev, A. Influence of substituents and ligands of various cobalt (II) porphyrin derivatives coordinately bonded to silica on the oxidation of mercaptan. *J. Mol. Catal. A: Chem.* **1993**, *80*, 253−267.
(27) Lü, H.; Zhang, Y.; Jiang, Z.; Li, C. Aerobic oxidative desulfurization of benzothiophene, dibenzothiophene and 4,6-dimethyldibenzothiophene using an Anderson-type catalyst $[(C_{18}H_{37})_2N(CH_3)_2]_5[IMo_6O_{24}]$. *Green Chem.* **2010**, *12*, 1954−1958.
(28) Lü, H.; Ren, W.; Liao, W.; Chen, W.; Li, Y.; Suo, Z. Aerobic oxidative desulfurization of model diesel using a B-type Anderson catalyst $[(C_{18}H_{37})_2N(CH_3)_2]_3Co(OH)_6Mo_6O_{18}\bullet 3H_2O$. *Appl. Catal., B* **2013**, *138*−*139*, 79−83.
(29) Kamata, K.; Sugahara, K.; Kato, Y.; Muratsugu, S.; Kumagai, Y.; Oba, F.; Hara, M. Heterogeneously catalyzed aerobic oxidation of sulfides with a $BaRuO_3$ nanoperovskite. *ACS Appl. Mater. Interfaces* **2018**, *10*, 23792−23801.
(30) Liu, M.; He, J.; Wu, P.; Lu, L.; Wang, C.; Chen, L.; Hua, M.; Zhu, W.; Li, H. Carbon nitride mediated strong metal−support interactions in a Au/TiO_2 catalyst for aerobic oxidative desulfurization. *Inorg. Chem. Front.* **2020**, *7*, 1212−1219.
(31) Wang, C.; Jiang, W.; Chen, H.; Zhu, L.; Luo, J.; Yang, W.; Chen, G.; Chen, Z.; Zhu, W.; Li, H. Pt nanoparticles encapsulated on V_2O_5 nanosheets carriers as efficient catalysts for promoted aerobic oxidative desulfurization performance. *Chin. J. Catal.* **2021**, *42*, 557−562.
(32) Wu, P.; Wu, Y.; Chen, L.; He, J.; Hua, M.; Zhu, F.; Chu, X.; Xiong, J.; He, M.; Zhu, W.; Li, H. Boosting aerobic oxidative desulfurization performance in fuel oil via strong metal-edge interactions between Pt and h-BN. *Chem. Eng. J.* **2020**, *380*, 122526.
(33) Zhang, M.; Liao, W.; Wei, Y.; Wang, C.; Fu, Y.; Gao, Y.; Zhu, L.; Zhu, W.; Li, H. Aerobic oxidative desulfurization by nanoporous tungsten oxide with oxygen defects. *ACS Appl. Nano Mater.* **2021**, *4*, 1085−1093.
(34) Dooley, K. M.; Liu, D.; Madrid, A. M.; Knopf, F. C. Oxidative desulfurization of diesel with oxygen: Reaction pathways on supported metal and metal oxide catalysts. *Appl. Catal., A* **2013**, *468*, 143−149.
(35) Jiang, W.; Gao, X.; Dong, L.; Xiao, J.; Zhu, L.-H.; Chen, G.-Y.; Xun, S.-H.; Peng, C.; Zhu, W.-S.; Li, H.-M. Aerobic oxidative desulfurization via magnetic mesoporous silica-supported tungsten oxide catalysts. *Pet. Sci.* **2020**, *17*, 1422−1431.
(36) Demir, E.; Mirzayev, M. N.; Tuğrul, A. B.; Abdurakhimov, B. A.; Karaaslan, S. İ. An experimental study on microstructure of tungsten alloys. *Surf. Rev. Lett.* **2020**, *27*, 1950169.
(37) Toth, L. E. *Transition Metal Carbides and Nitrides*; Academic Press: New York, 1971.
(38) Levy, R. B.; Boudart, M. Platinum-like behavior of tungsten carbide in surface catalysis. *Science* **1973**, *181*, 547−549.
(39) Rahsepar, M.; Pakshir, M.; Nikolaev, P.; Safavi, A.; Palanisamy, K.; Kim, H. Tungsten carbide on directly grown multiwalled carbon nanotube as a co-catalyst for methanol oxidation. *Appl. Catal., B* **2012**, *127*, 265−272.
(40) Yang, X. G.; Wang, C. Y. Nanostructured tungsten carbide catalysts for polymer electrolyte fuel cells. *Appl. Phys. Lett.* **2005**, *86*, 224104.
(41) McIntyre, D. R.; Burstein, G. T.; Vossen, A. Effect of carbon monoxide on the electrooxidation of hydrogen by tungsten carbide. *J. Power Sources* **2002**, *107*, 67−73.
(42) Brady, C. D. A.; Rees, E. J.; Burstein, G. T. Electrocatalysis by nanocrystalline tungsten carbides and the effects of codeposited silver. *J. Power Sources* **2008**, *179*, 17−26.
(43) Akopyan, A. V.; Polikarpova, P. D.; Forofontova, O. I.; Levin, I. S.; Mnatsakanyan, R. A.; Davtyan, D. A.; Zurnachyan, A. R.; Anisimov, A. V.; Karakhanov, E. A. Hydrogenation of alkenes on

https://doi.org/10.1021/acsomega.1c06969
ACS Omega 2022, 7, 11788−11798

molybdenum and tungsten carbides. *Theor. Found. Chem. Eng.* **2020**, *54*, 1045−1051.
(44) Mnatsakanyan, R.; Davtyan, D.; Zurnachyan, A.; Kharatyan, S.; Karakhanov, E.; Akopyan, A.; Manukyan, K. Microwave-assisted preparation and characterization of nanoscale rhenium diboride. *Ceram. Int.* **2018**, *44*, 22339−22344.
(45) Davtyan, D.; Mnatsakanyan, R.; Liu, L.; Aydinyan, S.; Hussainova, I. Microwave synthesis of B4C nanopowder for subsequent spark plasma sintering. *J. Mater. Res. Technol.* **2019**, *8*, 5823−5832.
(46) Joo, J. B.; Kim, J. S.; Kim, P.; Yi, J. Simple preparation of tungsten carbide supported on carbon for use as a catalyst support in a methanol electro-oxidation. *Mater. Lett.* **2008**, *62*, 3497−3499.
(47) He, C.; Tao, J.; Ke, Y.; Qiu, Y. Graphene-supported small tungsten carbide nanocrystals promoting a Pd catalyst towards formic acid oxidation. *RSC Adv.* **2015**, *5*, 66695.
(48) Ma, Y.-R.; Lin, C.-M.; Yeh, C.-L.; Huang, R.-T. Synthesis and characterization of one-dimensional WO_2 nanorods. *J. Vac. Sci. Technol., B: Microelectron. Nanometer Struct.–Process., Meas., Phenom.* **2005**, *23*, 2141−2145.
(49) Chen, P.; Qin, M.; Chen, Z.; Jia, B.; Qu, X. Solution combustion synthesis of nanosized WO_x: characterization, mechanism and excellent photocatalytic properties. *RSC Adv.* **2016**, *6*, 83101−83109.
(50) Lu, J. L.; Li, Z. H.; Jiang, S. P.; Shen, P. K.; Li, L. Nanostructured tungsten carbide/carbon composites synthesized by a microwave heating method as supports of platinum catalysts for methanol oxidation. *J. Power Sources* **2012**, *202*, 56−62.
(51) Yang, B. Q.; Wang, X. P.; Zhang, H. X.; Wang, Z. B.; Feng, P. X. Effect of substrate temperature variation on nanostructured WC films prepared using HFCVD technique. *Mater. Lett.* **2008**, *62*, 1547−1550.
(52) Szymańska-Kolasa, A.; Lewandowski, M.; Sayag, C.; Djéga-Mariadassou, G. Comparison of molybdenum carbide and tungsten carbide for the hydrodesulfurization of dibenzothiophene. *Catal. Today* **2007**, *119*, 7−12.
(53) Won, H. I.; Nersisyan, H. H.; Won, C. W. Combustion synthesis of nano-sized tungsten carbide powder and effects of sodium halides. *J. Nanopart. Res.* **2010**, *12*, 493−500.
(54) Debalina, B.; Kamaraj, M.; Murthy, B. S.; Chakravarthi, S. R.; Sarathi, R. Generation and characterization of nano-tungsten carbide particles by wire explosion process. *J. Alloys Compd.* **2010**, *496*, 122−128.
(55) Hoffmann, P.; Galindo, H.; Zambrano, G.; Rincón, C.; Prieto, P. FTIR studies of tungsten carbide in bulk material and thin film samples. *Mater. Charact.* **2003**, *50*, 255−259.
(56) Vijayalakshmi, R.; Jayachandran, M.; Sanjeeviraja, C. Structural, electrochromic and FT-IR studies on electrodeposited tungsten trioxide films. *Current Appl. Phys.* **2003**, *3*, 171−175.
(57) Nayak, B. B.; Dash, T.; Pradhan, S. Spectroscopic evaluation of tungsten carbide-titanium carbide composite prepared by arc plasma melting. *J. Electron Spectrosc. Relat. Phenom.* **2020**, *245*, 146993.
(58) Zhang, W.; Zhang, H.; Xiao, J.; Zhao, Z.; Yu, M.; Li, Z. Carbon nanotube catalysts for oxidative desulfurization of a model diesel fuel using molecular oxygen. *Green Chem.* **2014**, *16*, 211−220.
(59) Singh, B.; Smith, S. J.; Jensen, D. S.; Jones, H. F.; Dadson, A. E.; Farnsworth, P. B.; Vanfleet, R.; Farrer, J. K.; Linford, M. R. Multi-instrument characterization of five nanodiamond samples: a thorough example of nanomaterial characterization. *Anal. Bioanal. Chem.* **2016**, *408*, 1107−1124.
(60) Moulder, J. F.; Stickle, W. F.; Sobol, P. E.; Bomben, K. D. *Handbook of X-Ray Photoelectron Spectroscopy*; Perkin-Elmer Corp: Eden Prairie, Minnesota, USA, 1992.
(61) Wagner, C. D.; Naumkin, A. V.; Kraut-Vass, A.; Allison, J. W.; Powell, C. J.; Rumble, C. J. *NIST X-ray photoelectron spectroscopy database: NIST standard reference database 20*, Version 3.5. National Institute of Standards and Technology: Gaithersbg, 2003.
(62) Luthin, J.; Linsmeier, C. Influence of oxygen on the carbide formation on tungsten. *J. Nucl. Mater.* **2001**, *290-293*, 121−125.
(63) Chen, L.; Yi, D.; Wang, B.; Liu, H.; Wu, C. Mechanism of the early stages of oxidation of WC-Co cemented carbides. *Corros. Sci.* **2016**, *103*, 75−87.
(64) Guozuan, X.; Liu, R.; Qiumin, Y.; Chenghui, Y.; Guohui, H.; Xiang, X. Preparation and characterization of Cr-doped tungsten oxide by liquid-liquid doping precursor. *Mater. Res. Express* **2021**, *8*, 016509.
(65) Rodríguez Ripoll, M.; Totolin, V.; Gabler, C.; Bernardi, J.; Minami, I. Diallyl disulphide as natural organosulphur friction modifier via the in-situ tribo-chemical formation of tungsten disulphide. *Appl. Surf. Sci.* **2018**, *428*, 659−668.
(66) Nakazawa, M.; Okamoto, H. Surface composition of prepared tungsten carbide and its catalytic activity. *Appl. Surf. Sci.* **1985**, *24*, 75−86.
(67) Fenoglio, I.; Tomatis, M.; Lison, D.; Muller, J.; Fonseca, A.; Nagy, J. B.; Fubini, B. Reactivity of carbon nanotubes: Free radical generation or scavenging activity? *Free Radicals Biol. Med.* **2006**, *40*, 1227−1233.
(68) Eseva, E. A.; Lukashov, M. O.; Cherednichenko, K. A.; Levin, I. S.; Akopyan, A. V. Heterogeneous catalysts containing an Anderson-type polyoxometalate for the aerobic oxidation of sulfur-containing compounds. *Ind. Eng. Chem. Res.* **2021**, *60*, 14154−14165.
(69) Irani, M.; Fan, M.; Ismail, H.; Tuwati, A.; Dutcher, B.; Russell, A. G. Modified nanosepiolite as an inexpensive support of tetraethylenepentamine for CO_2 sorption. *Nano Energy* **2015**, *11*, 235−246.
(70) Li, X.; Gu, Y.; Chu, H.; Ye, G.; Zhou, W.; Xu, W.; Sun, Y. MFM-300(V) as an active heterogeneous catalyst for deep desulfurization of fuel oil by aerobic oxidation. *Appl. Catal., A* **2019**, *584*, 117152.
(71) Wang, C.; Qiu, Y.; Wu, H.; Yang, W.; Zhu, Q.; Chen, Z.; Xun, S.; Zhu, W.; Li, H. Construction of 2D-2D V_2O_5/BNNS nanocomposites for improved aerobic oxidative desulfurization performance. *Fuel* **2020**, *270*, 117498.

https://doi.org/10.1021/acsomega.1c06969
ACS Omega 2022, 7, 11788−11798